A compliant four-bar linkage mechanism that makes the fingers of a prosthetic hand more impact resistant

Kyung Yun Choi[1], Aadeel Akhtar[2] and Timothy Bretl[1]

***Abstract*— Repeated mechanical failure due to accidental impact is one of the main reasons why people with upper-limb amputations abandon commercially-available prosthetic hands. To address this problem, we present the design and evaluation of a compliant four-bar linkage mechanism that makes the fingers of a prosthetic hand more impact resistant. Our design replaces both the rigid input and coupler links with a monolithic compliant bone, and replaces the output link with three layers of pre-stressed spring steel. This design behaves like a conventional four-bar linkage but adds lateral compliance and eliminates a pin joint, which is a main site of failure on impact. Results from free-end and fixed-end impact tests show that, compared to those made with a conventional four-bar linkage, fingers made with our design absorb up to 52% more energy on impact with no mechanical failure. We also show the integration of these fingers in a prosthetic hand that is low-cost, light-weight, and easy to assemble, and that has grasping performance comparable to commercially-available hands.**

I. Introduction

Repeated mechanical failure due to accidental impact is a leading cause of prosthesis abandonment by people with upper-limb amputations [1]. Consequently, surveys have shown that people with upper limb amputations place high priority on the need for their prostheses to be impact resistant [2]. In fact, a study by Biddiss, et al. [3] reported 91% of surveyed people with upper limb amputations who rejected their prostheses stated a lack of impact resistance as the primary reason for rejection, despite having advanced functions like myoelectric control and multi-articulated fingers in their prosthetic hand. The problem of mechanical failure due to a lack of impact resistance is even more apparent with workers in jobs that require intense manual labor, who frequently forgo the use of advanced myoelectric prostheses because they are more susceptible to becoming damaged [4].

Despite the reported need for prosthetic hands that are impact resistant, few studies have focused on this measure of performance. In the past five years, researchers have worked to increase impact resistance in robotic hands by introducing compliance, such as in the iHY hand [5] and the PISA/IIT Soft hand [6]. The impact resistance of these hands were evaluated through qualitative methods, such as striking the fingers with a blunt instrument and showing that the hand still functions properly. The DLR hand [7] was one of the few in which impact resistance was evaluated quantitatively by measuring the energy absorbed by a finger upon impact on the dorsal side of the finger.

[1]Kyung Yun Choi and Timothy Bretl are with the Dept. of Aerospace Engineering, [2]Aadeel Akhtar is with the Neuroscience Program and Medical Scholars Program, University of Illinois at Urbana-Champaign, Urbana, IL 61801, USA {kchoi19, tbretl, aakhta3}@illinois.edu

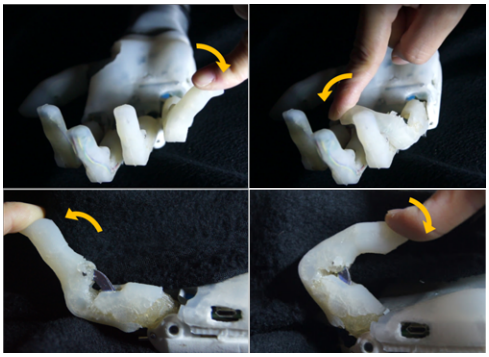

Fig. 1. Our four-bar linkage driven-finger is compliant and resistant to impacts from multiple directions.

In this paper, we present the design and evaluation of a compliant four-bar linkage mechanism that makes the fingers of a prosthetic hand more impact resistant (Fig. 1). Four-bar linkages are widely used in robotic fingers (e.g. TBM, Remedi, Tact, SSSA-MyHand) [8]–[10]. Most commercial prosthetic hands, in particular, use fingers with four-bar linkages (e.g. Vincent, iLimb, Bebionic) [11]. Our design replaces both the rigid input and coupler links with a monolithic compliant bone, and replaces the output link with three layers of pre-stressed spring steel. This design behaves like a conventional four-bar linkage but adds lateral compliance and eliminates a pin joint, which is a main site of failure on impact. We performed free-end and fixed-end impact tests to evaluate the impact resistance of our compliant four-bar linkage mechanism, measuring the energy absorbed from impact on the volar, dorsal, and lateral aspects of the finger. In addition, we characterize the compliance of our finger through static load tests, and fingertip force measurements.

In this paper, we also show how to integrate our finger design in a myoelectric prosthetic hand that is mobile, compact (50th percentile female anthropometry), light-weight (312 g), inexpensive ($553 in raw materials [12]), and easy to assemble due to reduced components. We show that our hand can easily grasp household objects through the use of our compliant finger design. Furthermore, we can easily attach it to a socket, and have recently applied it to a patient with an upper-limb amputation who was able to use it to perform fine sensorimotor control tasks [12]. Finally, all the materials, designs, and files used to make the hand can be found on our website[†], and step-by-step instructions on building the hand can be found on the Instructables website[‡].

[†]http://bretl.csl.illinois.edu/prosthetics

[‡]http://www.instructables.com/id/Compliant-Prosthetic-Hand-With-Sensorimotor-Contro/

Finally, it should be noted that we could have taken a different approach by designing a tendon-driven compliant finger, as done in the DLR hand [7], the iHY hand [5], the UB Hand IV [13], and the PISA/IIT Soft hand [6]. However, we chose to focus on making a compliant four-bar linkage-driven finger since it is common in robotic finger designs and most commercial prosthetic hands.

II. Methods

A. Compliant Finger Design

Fig. 2a shows the overall design of our compliant finger. We followed the following five design principles:

1) Develop a monolithic structure, minimizing the number of physical joints to reduce areas vulnerable to impact: By using a monolithic finger design, we replace the revolute pin in the proximal interphlangeal (PIP) joint (joint B) of the standard four-bar linkage mechanism (Fig. 2b) with a compliant joint (joint B in Fig. 2a). Making the PIP joint compliant has several advantages over a standard four-bar linkage, including no energy loss to friction, no need for lubrication, no hysteresis, easier fabrication, and virtually no need for maintenance [14]. The monolithic bone helps reduce the weight of the finger, while also enabling torsional and flexural compliance.

2) Embed the links in a soft skin: Our design allows the monolithic bone to be enveloped in a soft silicone skin through a single molding process. Using soft materials has advantages in attenuation of impact forces, conformability, and repetitive strain dissipation [15].

3) Design the proximal interphalangeal (PIP) joint to have variable compliance: While compliance allows the PIP joint to better absorb energy on high impacts, there is a tradeoff in its ability to hold static loads. Consequently, we designed the PIP joint to have variable compliance depending on the direction the load is being applied by constructing different spring mesh models. A simplified spring model of the compliant joint in the sagittal plane is shown in Figs. 2c-2e. When the finger flexes, the external force is applied to node 1; when the finger extends, the external force is applied to node 5.

4) Design the metacarpophalangeal (MCP) and distal interphalangeal (DIP) joints to be compliant: In addition to making the PIP joint compliant, we made the MCP and DIP joints compliant as well. The MCP joint can be modeled as a torsional spring and its stiffness is denoted as k_{in}. When no load is applied, the DIP joint angle is at 20°, but compliance allows the joint angle to vary when loaded via elastic deformation.

5) Design an output link to be impact-resistant to lateral forces: We used three pieces of blue-tempered spring steel (Fig. 2f) to construct the output link. The design enables the finger to be compliant to lateral forces, but rigid in the flexion/extension direction to handle heavy loads. The two outer pieces of steel are pre-stressed to form a symmetric curvature that allows the link to quickly recover to its initial state, restoring more energy upon impact.

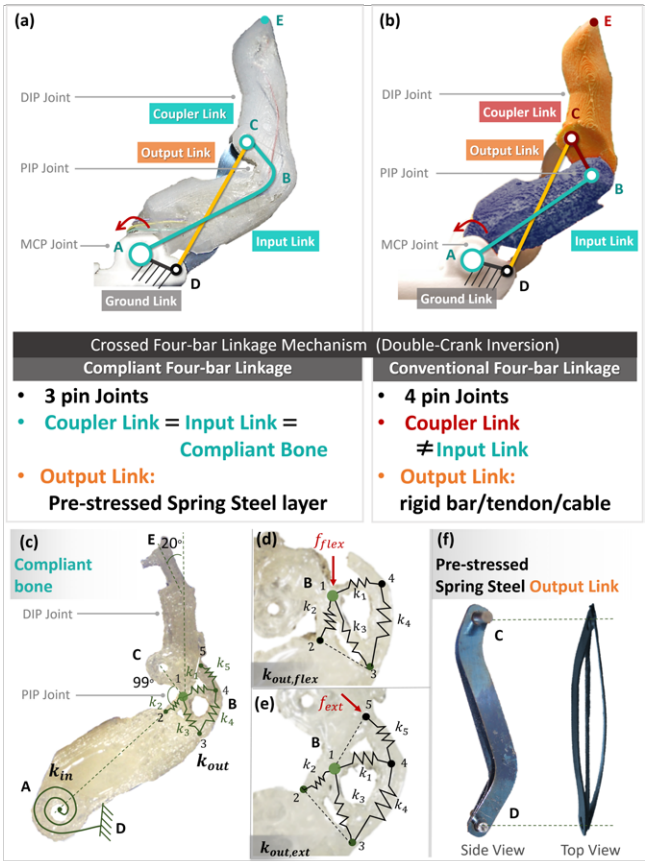

Fig. 2. (a) Compliant four-bar linkage mechanism (b) Conventional four-bar linkage mechanism (c) 3-D printed polyurethane bone structure. The angle between $\overline{AB}$ and $\overline{BC}$ is pre-defined to be 99°. The DIP joint angle is 20°. Node 1 represents the joint B. (b) Flexion spring elements model of compliant PIP joint. (c) Extension spring elements model of compliant PIP joint. (d) Output link consists of three blue-tempered spring steels.

B. Four-bar Linkage

The lengths of each link in our four-bar linkage (Fig. 2a) are: ground link $= \overline{AD} = 8.55$ mm, input link $= \overline{AB} = 37.11$ mm, coupler link $= \overline{BC} = 8.78$ mm, output link $= \overline{CD} = 37.04$ mm, $\overline{CE} = 32.77$ mm, $\overline{BE} = 40.38$ mm. The relationship between links satisfies the double-crank inversion defined by the Grashof condition. The range of motion is 105.0° for the MCP joint and 93.0° for the PIP joint. With respect to the MCP joint, the range of motion of the fingertip is 154.4° when no load is applied. Our finger has the largest range of motion compared to the four commercial prosthetic hands and eleven research hands described in Belter, et al. [8]. The MCP joint is directly actuated by a motor mated to a worm gear train. The MCP, PIP, and DIP joints are coupled by linkages.

C. Fabrication

Fabrication consists of two parts: building a monolithic bone structure (Figs. 3a-3d) and molding a silicone skin (Figs. 3e-3j). The monolithic bone is 3-D printed (Replicator 2X, MakerBot) using a flexible thermoplastic polyurethane filament (SemiFlex, NinjaTek). Two MEMS barometric pressure sensors (MPL115A2, Freescale, Inc.) are embedded in the distal fingertip of the bone, used to detect contact forces

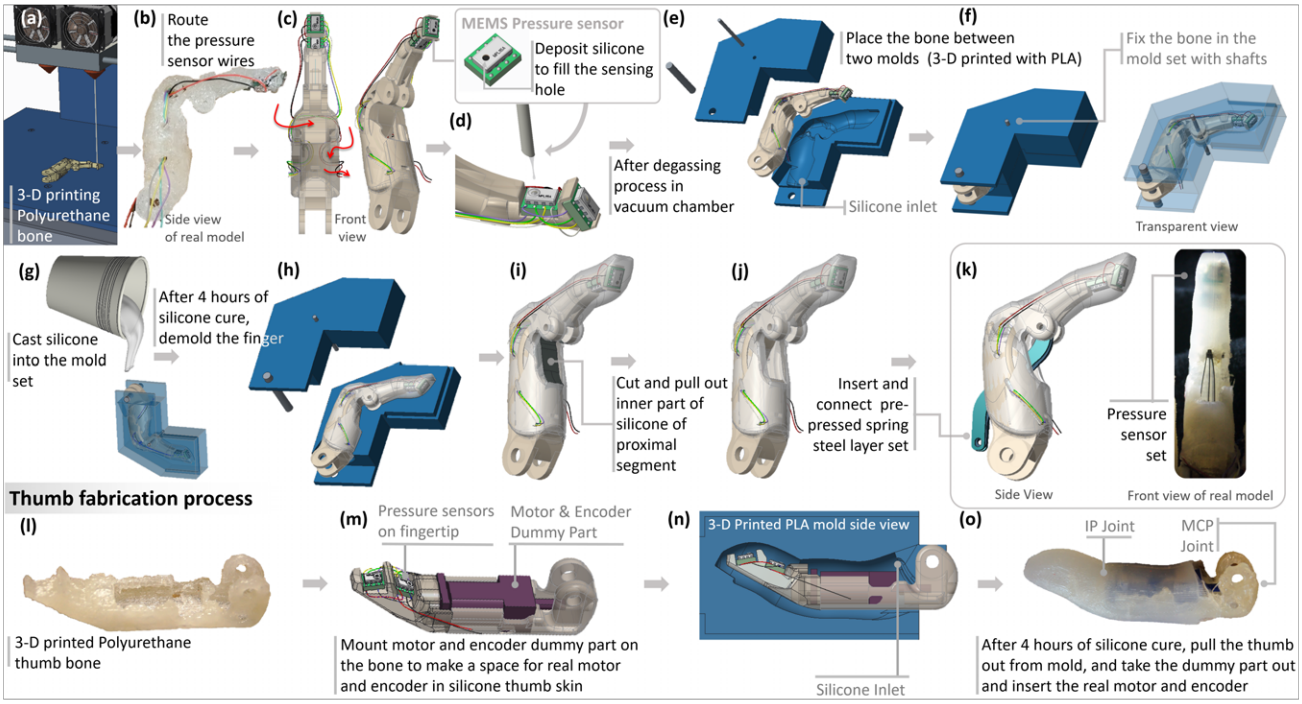

Fig. 3. The fabrication process for the fingers and thumb with embedded barometric pressure sensors.

perpendicular to the fingertip surface [16]. In order to detect contact forces, the sensing hole of the pressure sensor is filled with silicone (Dragon Skin 20, Smooth-On, Inc.). Next, the bone with the pressure sensors is inserted between two 3-D printed molds (Fig. 3e). After cutting a hole in the silicone skin (Fig. 3i), the pre-stressed spring steel layers are connected to joint C (Fig. 2a) and the ground joint (joint D, Fig. 2a) of the dorsal palm (Figs. 3j-3k).

Figs. 3l-3o show the process of fabricating the thumb. The thumb bone is constructed of the same polyurethane material as the fingers. The interphalangeal (IP) joint of the thumb is set to 20° as in the DIP joints of the other four fingers.

The palm is 3-D printed in two pieces (dorsal and volar) using polylactic acid (PLA) filament. The volar palm is embedded in silicone (EcoFlex 30, Smooth-On, Inc.) and snap-fits on to the dorsal palm.

III. Performance Analysis

A. Impact Resistance

The maximum contact force and impact energy during structural deformation are used to evaluate the impact resistance of a structure [17]. We use these measures to evaluate the impact resistance of our compliant finger with a compliant PIP joint (Fig. 4a), and compare it to a compliant finger using a pin for the PIP joint (Fig. 4b), a finger with a rigid MCP joint using a pin for the PIP joint (Fig. 4c), and a 1045 HR steel bar having the same length and thickness of the fingers and is used as a reference. We also observed the effects of the impact on the finger structure, motor, and worm gear set to identify locations of any mechanical failure.

We conducted free-end and fixed-end impact tests using a standard impact test machine (Dynatup 8250, Instron, Inc.). The finger was attached to a motor (100:1 Micro Metal Gearmotor 6V HPCB, Pololu, Inc.) and a worm gear set, rigidly attached to the testbed of the impact test machine. The fixed-end impact test simulated accidents involving the finger being stuck between two objects, such as a door hinge. The free-end impact test simulated accidents involving the finger receiving high-speed impacts from a blunt object, such as a hammer.

In each test, a weight was dropped on the volar, dorsal, and lateral aspects of the finger. We control the impact velocity by varying the height at which the weight is dropped. We varied both the drop height and mass of the weight until we reached the maximum of the range or structural failure occurred. The range of masses used for the weight was 3.44 kg-5.99 kg. The range of the drop height was 20 mm-905 mm. Only the free-end impact test was performed on the steel bar and the rigid MCP joint finger with a pin PIP joint. We recorded the impact velocity (v_i) and impact load with respect to time ($p(t)$), obtained from the impact test machine's load cell. We computed the impact energy ($E_{impact}(t)$) as follows,

$$E_{impact}(t) = \frac{m}{2}(v_i^2 - v(t)^2) + mgx(t),$$

where m is the mass of the weight, g is the gravitational constant, $v(t)$ is the velocity of the weight and is equal to $\int_{t_i}^{t}(g - \frac{p(t)}{m})\,\mathrm{d}t + v_i$, and $x(t)$ is the deformation of the finger, equal to $\int_{t_i}^{t} v(t)\,\mathrm{d}t$.

Table I compares the maximum impact load and impact energy of the fingers. In the free-end impact test, the compliant finger with a pin PIP joint and the rigid MCP joint finger with a pin PIP joint were subject to mechanical failure when the mass of the weight was 3.34 kg. For the compliant finger

TABLE I
IMPACT TEST RESULTS

Mass of weight: 5.99 kg Drop height: 905 mm	Free-end Impact Test						Fixed-end Impact Test			
	Volar		Dorsal		Lateral		Volar		Lateral	
	Max. Impact Load [kN]	Max. Impact Energy [J]	Max. Impact Load [kN]	Max. Impact Energy [J]	Max. Impact Load [kN]	Max. Impact Energy [J]	Max. Impact Load [kN]	Max. Impact Energy [J]	Max. Impact Load [kN]	Max. Impact Energy [J]
Compliant finger with compliant PIP joint	1.23	23.06	1.84	24.48	1.55	10.74	1.20	22.36	1.45	13.46
Compliant finger with pin PIP joint	1.26†	6.27†	1.62*	22.23*	0.94†	7.05†	0.65*	21.97*	2.32*	13.16*
Rigid MCP joint finger with pin PIP joint	0.07‡	0.10‡	0.07‡	0.60‡	0.04‡	0.28‡	—	—	—	—
1045 HR steel bar	9.93†	21.26†	—	—	—	—	—	—	—	—

Structural failure at (drop weight, drop height): †(3.34 kg, 465 mm), ‡(3.34 kg, 20 mm), *(5.99 kg, 905 mm)

with a pin PIP joint, the impact caused dislocation of the PIP joint and misaligned the MCP joint with the worm gear set. For the rigid MCP joint finger with a pin PIP joint, the impact caused a fracture in the proximal segment around the PIP joint with an impact velocity of 0.64 m/s. The 1045 HR steel bar showed plastic deformation when the mass of the weight was 3.34 kg and the drop height was 465 mm. It had the highest measured impact load at 9.93 kN, but absorbed less impact energy than the compliant finger with a compliant PIP joint. We did not detect any mechanical damage in the compliant finger with a compliant PIP joint during the free-end impact test in any of the three directions at the maximum mass of 5.99 kg at the highest drop height of 905 mm. At the highest impact velocity of 4.15 m/s, the compliant finger with a compliant PIP joint absorbed 11%-52% more impact energy than the fingers with a pin PIP joint.

In the fixed-end impact test, the compliant finger with a pin PIP joint was subject to mechanical failure when the mass of the weight was 5.99 kg and the drop height was 905 mm. The impact damaged the PIP joint and distal finger segment. Again, the compliant finger with a compliant PIP joint absorbed the highest impact energy without failure in the fixed-end impact test. The impact test results show that the compliant finger with a compliant PIP joint can withstand higher impacts from the volar, dorsal and lateral directions by absorbing more impact energy than the other fingers. Because the compliant finger with a compliant PIP joint never failed mechanically, it is able to protect the actuator and gear train from damage, as shown in video†.

B. Fingertip Force

We measured the force generated from the fingertip using a calibrated force sensitive resistor (FlexiForce®, Tekscan, Inc.). We used the same fingers from the impact tests for comparison (Figs. 4a-4c). We recorded the force normal to the fingertip as the finger flexed until its motor stalled. We performed each test four times, averaging the the maximum force values from each trial. The results are shown in Table II. We also compared our results to those of the iLimb Small, iLimb Pulse Small, Vincent Small, and Bebionic Small hands which are comparable to ours with respect to size [11]. We computed the gear ratio of the motor to the MCP joint by multiplying the gearbox ratio of the DC motor (100:1) by the worm gear reduction ratio (20:1).

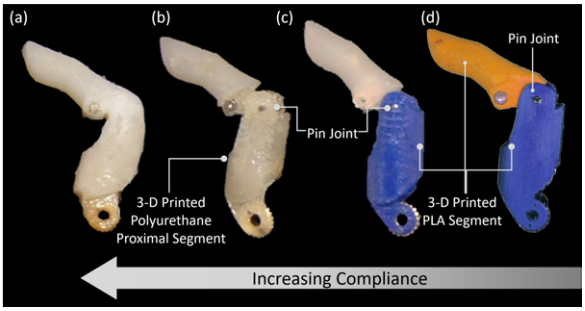

Fig. 4. (a) Compliant finger with compliant PIP joint. (b) Compliant finger with pin PIP joint. (c) Rigid MCP joint finger with pin PIP joint. The proximal segment of the finger is rigid and made of 3-D printed PLA. (d) Rigid finger with pin joint. The proximal and distal segments are rigid and made of 3-D printed PLA. All the pin joints are connected by a 2 mm diameter stainless steel shaft and two plastic shaft sleeves.

Of the fingers we tested, the rigid MCP joint finger with a pin PIP joint exerted the smallest fingertip force (3.48 N) followed by the compliant finger with a pin PIP joint (4.92 N). The compliant finger with a compliant PIP joint generated the highest fingertip force (5.86 N). Since all three of the fingers tested used the same motor, they had the same input torque. Consequently, the differences in fingertip force are due solely to mechanical amplification from displacement of the fingertip [14].

C. Compliance of PIP Joint

We evaluated the compliance of the compliant PIP joint by applying loads normal to the fingertip between 163 g-1051 g in both the flexion and extension directions. We determined the relationship between the displacement of the PIP joint angle and the applied force, shown in Fig. 5. The slope of the red curve is the compliance of the PIP joint as the finger flexed, and the slope of the blue curve is the compliance when the finger extended. The compliance of the PIP joint when the fingers flexed was larger than when the fingers extended. These results confirm that the compliance of the PIP joint is dependent on the direction the load is applied, which allows the finger to be more energy efficient when flexing but hold a greater static load as it extends.

IV. ASSEMBLED PROSTHETIC HAND

A. Hand Design

The fully assembled hand has six degrees-of-freedom corresponding to flexion/extension in the five digits and

TABLE II

FINGERTIP FORCE AND MOTOR COMPARISON

Finger	Motor	Motor Price (USD)	Motor Stall Torque [mNm]	Gear Ratio, Motor to MCP joint	Average Fingertip Force (N)	Std. Dev.	No. of Trials
Compliant finger with compliant PIP joint	Pololu 100:1 HPCB	18.95	2.16	2000:1	5.86	0.2	4
Compliant finger with pin PIP joint	Pololu 100:1 HPCB	18.95	2.16	2000:1	4.92	0.2	4
Rigid MCP joint finger with pin PIP joint	Pololu 100:1 HPCB	18.95	2.16	2000:1	3.48	0.2	4
iLimb Small [11]	Maxon RE 10 118394	72.88	3.04	1600:1	5.17	0.1	2
iLimb Pulse Small [11]	Maxon RE 10 118394	72.88	3.04	1600:1	4.09 or 8.56*	0.1	2
Vincent Small [11]	Maxon 1017	-	-	-	3.00	0.1	2
Bebionic Small [11]	Faulhaber 1024M006SR	-	2.34	-	16.11	0.2	2

*Holding force after pulse mode.

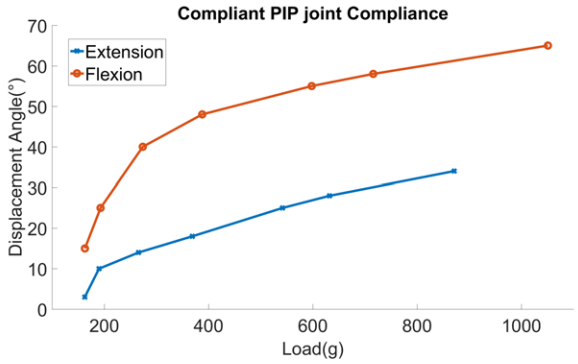

Fig. 5. Plot showing load (g) versus compliant PIP joint rotational displacement (°) in the flexion and extension directions in the compliant finger (with a detached Output Link).

thumb rotation. Fig. 6a shows six 100:1 HPCB Pololu Micro Metal Gearmotors mated to a single-envelope worm gear (module = 0.5) and worm transmission, which enables non-backdrivable actuation important for energy efficiency. The prosthetic hand has 50th percentile female hand anthropometry (Fig. 6b). The total weight of the hand is 312 g (340 g with the wrist connection bolt) which is less than the average weight of the human hand (400 g) [18]. People with upper limb amputations can control the hand using electromyographic pattern recognition, and can feel contact pressure through electrotactile sensory substitution transduced from the fingertip pressure sensors, described in Akhtar, et al. [12].

B. Static Load Test

We measured the maximum static load capacity of a fully extended individual finger, of the assembled hand making a power grasp, and of the assembled hand fully open. All tests were done using the compliant finger with a compliant PIP joint design. For the individual finger test, the motor of the finger was clamped to a table, and a bag holding a variable amount of weight was hooked on to the PIP joint with the weight increasing in increments of 2.26 kg. For the power grasp test, the bag with the weight was placed on the floor, and the hand had to lift the bag 15 cm vertically for ∼10 s. For hand fully open test, the hand was clamped to the table in a supine position and the bag with the weight was hooked on to the proximal segments of the index, middle, ring, and little fingers. When the applied load was larger than the maximum load the hand could hold, instead of causing

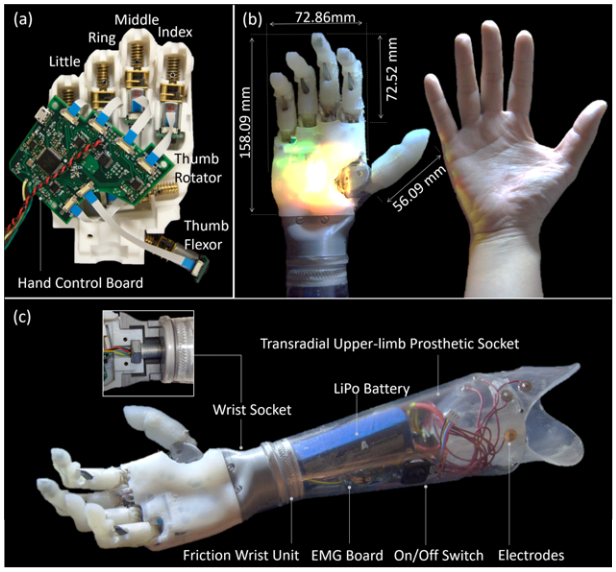

Fig. 6. (a) Six DC motors assembled on the 3-D printed dorsal palm. (b) The hand has 50th percentile female hand anthropometry. (c) The fully assembled hand attached to a socket for a person with a transradial amputation. The battery, electromyography (EMG) board, and electrodes all fit in the socket, enabling the hand to be mobile.

mechanical damage to actuator, gear train or hand structure, the MCP joint underwent rotational elastic deformation until the bag fell to the floor. The fingers were able to recover to their initial positions and shape after exceeding the maximum load capacity. The individual finger was able to hold up to 17.23 kg, the power grasp was able to hold up to 23.06 kg, and the fully open hand was able to hold up to 26.22 kg. A video showing these results can be found on our website[†].

C. Grasp Performance

To assess the functionality of our hand, we performed a grasping test in which we had the hand grasp common household items. We compared the performance of our hand using compliant fingers with a compliant PIP joint (Fig. 4a) to an assembled hand using rigid fingers with a pin PIP joint (Fig. 4d). Depending on the object, the hand made the appropriate grasp (key, three-jaw chuck, or power) to hold the item. For the compliant hand, the compliance of the fingers allowed the hand to grasp various types of objects by conforming to the shape of the object (Fig. 7). The compliant

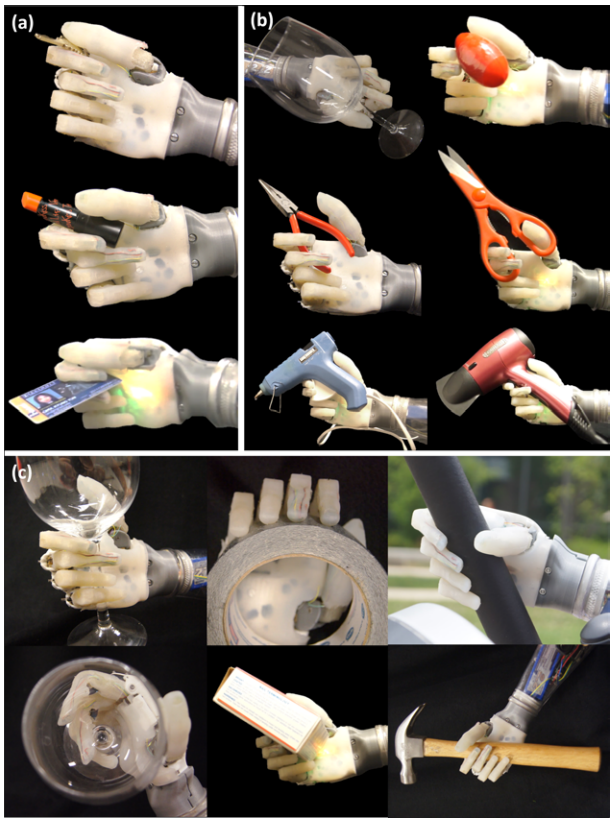

Fig. 7. (a) Key grasp of a key and lipstick. The hand can also grasp a card between any of the fingers. (b) Three-jaw chuck grasp of a wine glass, egg-shaped plastic block, needle-nose pliers, scissors, hot glue gun, and a hair dryer. (c) Power grasp of a wine glass, duct tape, elliptical machine handlebar, wine glass (top view), small cardboard box, and a hammer.

hand also had the benefit of being able to grip different objects using the same grasp (e.g. power) but with different final finger positions. For example, as shown in Fig. 7c, when the hand grasped a roll of duct tape using a power grasp, the fingertips conformed to the curved surface of the tape. However, when the hand power grasped a small cardboard box, the fingertips formed a straight line on the flat surface of the box. As before, a video showing these results can be found on our website[†].

V. Conclusion

To improve impact resistance in prosthetic hands, we presented the design and evaluation of a compliant four-bar linkage mechanism used to make fingers that are mechanically robust. The finger consisted of 1) a monolithic compliant bone 3-D printed using polyurethane filament enabling torsional and flexural compliance, and 2) three layers of pre-stressed spring steel to form a compliant output link resistant to lateral impacts. Impact tests showed that our compliant finger design absorbed up to 52% more energy on impact when compared to fingers using a conventional four-bar linkage. There was no mechanical failure upon impact from a 5.99 kg weight with a maximum impact velocity of 4.15 m/s on the volar, dorsal, or lateral aspects of the finger. Our compliant finger generated up to 68% more fingertip force than a conventional four-bar linkage-driven finger. The fingers can be easily assembled into a hand that is mobile, low-cost ($553), light-weight (312 g), compact (50th percentile female anthropometry), can hold loads of up to 26 kg, and can easily grasp a variety of household objects. We can easily attach our hand to a socket, and have recently applied it to a patient with an upper-limb amputation [12]. All materials, designs, files and building instructions can be found on our website[†] and on the Instructables website[‡].

Acknowledgments

This work was supported by Korean Government Scholarship Program, NIH F30HD084201, and NSF IIS-1320519.

References

[1] K. Bhaskaranand, A. K. Bhat, and K. N. Acharya, "Prosthetic rehabilitation in traumatic upper limb amputees (an Indian perspective)," *Arch. Orthop. Trauma Surg.*, vol. 123, no. 7, pp. 363–366, 2003.

[2] U. Wijk and I. Carlsson, "Forearm amputees' views of prosthesis use and sensory feedback," *J. Hand Ther.*, vol. 28, no. 3, pp. 269–278, 2015.

[3] E. A. Biddiss and T. T. Chau, "Upper limb prosthesis use and abandonment: A survey of the last 25 years," *Prosthet. Orthot. Int.*, vol. 31, no. 3, pp. 236–257, 2007.

[4] F. Cordella, A. L. Ciancio, R. Sacchetti, A. Davalli, A. G. Cutti, E. Guglielmelli, and L. Zollo, "Literature review on needs of upper limb prosthesis users," *Front. Neurosci.*, vol. 10, p. 209, 2016.

[5] L. U. Odhner, L. P. Jentoft, M. R. Claffee, N. Corson, Y. Tenzer, R. R. Ma, M. Buehler, R. Kohout, R. D. Howe, and A. M. Dollar, "A compliant, underactuated hand for robust manipulation," *Int. J. Robot. Res.*, 2014.

[6] M. Catalano, G. Grioli, E. Farnioli, A. Serio, C. Piazza, and A. Bicchi, "Adaptive synergies for the design and control of the Pisa/IIT SoftHand," *Int. J. Robot. Res.*, vol. 33, no. 5, pp. 768–782, 2014.

[7] M. Grebenstein, M. Chalon, W. Friedl, S. Haddadin, T. Wimbck, G. Hirzinger, and R. Siegwart, "The hand of the DLR hand arm system: Designed for interaction," *Int. J. Robot. Res.*, vol. 31, no. 13, pp. 1531–1555, 2012.

[8] J. T. Belter and A. M. Dollar, "Performance characteristics of anthropomorphic prosthetic hands," in *IEEE Int. Conf. Rehabil. Robot.*, vol. 29. Citeseer, 2011, pp. 1–7.

[9] P. Slade, A. Akhtar, M. Nguyen, and T. Bretl, "Tact: Design and performance of an open-source, affordable, myoelectric prosthetic hand," in *IEEE Int. Conf. Robot Autom.*, May 2015, pp. 6451–6456.

[10] M. Controzzi, F. Clemente, D. Barone, A. Ghionzoli, and C. Cipriani, "The SSSA-MyHand: a dexterous lightweight myoelectric hand prosthesis," *IEEE Trans. Neural Syst. Rehabil. Eng.*, 2016.

[11] J. T. Belter, J. L. Segil, A. M. Dollar, and R. F. Weir, "Mechanical design and performance specifications of anthropomorphic prosthetic hands: A review." *J. Rehabil. Res. Dev.*, vol. 50, no. 5, 2013.

[12] A. Akhtar, K. Y. Choi, M. Fatina, J. Cornman, E. Wu, J. Sombeck, C. Yim, P. Slade, J. Lee, J. Moore, D. Gonzales, A. Wu, G. Anderson, D. Rotter, C. Shin, and T. Bretl, "A low-cost, open-source, compliant hand for enabling sensorimotor control for people with transradial amputations," in *Conf. Proc. IEEE Eng. Med. Biol. Soc.*, 2016.

[13] C. Melchiorri, G. Palli, G. Berselli, and G. Vassura, "Development of the UB Hand IV: Overview of design solutions and enabling technologies," *IEEE Robot. Autom. Mag.*, vol. 20, no. 3, pp. 72–81, Sept 2013.

[14] N. Lobontiu, *Compliant mechanisms: Design of flexure hinges*. CRC press, 2002.

[15] K. B. Shimoga and A. A. Goldenberg, "Soft materials for robotic fingers," in *IEEE Int. Conf. Robot Autom.*, 1992, pp. 1300–1305.

[16] Y. Tenzer, L. P. Jentoft, and R. D. Howe, "Inexpensive and easily customized tactile array sensors using MEMS barometers chips," *IEEE R&A Magazine*, 2012.

[17] W. J. Stronge, *Impact Mechanics*. Cambridge University Press, 2004.

[18] R. Chandler, C. E. Clauser, J. T. McConville, H. Reynolds, and J. W. Young, "Investigation of inertial properties of the human body," U.S. Department of Transportation, Tech. Rep. Report No. DOT HS-801 430, 1975.